Available online at www.sciencedirect.com
ScienceDirect
Journal of the European Ceramic Society 27 (2007) 2393–2400
www.elsevier.com/locate/jeurceramsoc

Prediction of the elastic properties profile in glass-alumina functionally graded materials

V. Cannillo, L. Lusvarghi, C. Siligardi, A. Sola *

Dipartimento di Ingegneria dei Materiali e dell'Ambiente, University of Modena and Reggio Emilia, Italy

Received 9 June 2006; received in revised form 12 September 2006; accepted 16 September 2006
Available online 24 October 2006

Abstract

Glass-alumina functionally graded materials were obtained by percolation and alternatively by plasma spraying. The paper develops a reliable model to predict the functional gradient of the analysed systems. A finite element code, which was able to handle microstructural images, was employed to estimate the effective elastic properties along the gradient direction. The calculated values were compared with experimental data acquired by means of systematic microindentation tests. The computational approach was compared with analytical tools such as the rule of mixture. The results revealed that the elastic properties were significantly influenced by microstructural features such as the shape of the ingredient materials domains and the presence of pores at the grain boundaries. This was particularly evident in the sprayed FGMs, due to their peculiar lamellar microstructure. Even if the coating–substrate interface properties were difficult to include in the model, the numerical simulations fitted fairly well the experimental data.

Keywords: Mechanical properties; Al_2O_3; Glass; Functionally graded materials

1. Introduction

Functionally graded materials (FGMs) are an innovative class of composite materials, characterized by an engineered spatial distribution of the constituent phases.[1] In fact, unlike traditional composite materials, FGM ingredient materials are not uniformly arranged in space, but are designed in order to provide a wanted compositional and/or microstructural gradient.[2] The smooth variation of composition and/or microstructure results in a gradient of properties, which can be tailored to the assigned thermo-mechanical loadings. FGMs, therefore, may be optimally applied whenever the service conditions are different from point to point.[3,4] Moreover, FGMs may be advantageous with respect to traditional bi-materials systems, where two different materials are abruptly coupled, since the gradual change of composition in FGMs may reduce the stress state at the interface.[4,5] Actually FGMs were first introduced in the 1980s in Japan as innovative high performance thermal barrier coatings for aerospace vehicles.[6]

Moreover, if the functional gradient is properly designed, the final FGM can show special properties, which cannot be achieved by the ingredient materials considered separately or a traditional composite material having the same mean composition as the FGM.[7,8] From this point of view, great attention has been paid to the effect of introducing a gradient in elastic properties on the indentation strength of materials. Giannakopoulos et al.[7] analysed glass-alumina graded coatings, characterized by a progressive increase of the Young's modulus with depth, and they demonstrated that the elastic gradient significantly improved the material resistance to elastic Hertzian indentation. Furthermore, Suresh et al.[8] proved that, if the spatial change of the elastic properties was optimised, the resistance to sliding-contact damage of such glass-alumina FGMs could be significantly improved.

FGMs are widely used whenever the applied thermo-mechanical loads vary with location within the same component, since the functional gradient can be tailored to the prescribed service conditions.[3,4] However, the material gradation, which induces the functional gradient, makes FGMs behave in a different way from homogeneous materials or traditional composites[7] and it is extremely difficult to understand the correlation existing between the microstructure of graded heterogeneous materials

* Corresponding author. Tel.: +39 059 2056240; fax: +39 059 2056243.
E-mail address: sola.antonella@unimo.it (A. Sola).

0955-2219/$ – see front matter © 2006 Elsevier Ltd. All rights reserved.
doi:10.1016/j.jeurceramsoc.2006.09.009

and their effective properties.[9,10] Therefore, since FGMs were first introduced, several models have been proposed to predict the resulting performances of graded systems on the basis of their composition and microstructure.[10–13]

In the present work, a microstructure-based finite element method (FEM) was applied to glass-alumina FGMs with the aim of evaluating their effective elastic gradient, which governs their superficial resistance. Two different production techniques were utilized, i.e. percolation and plasma spraying. The former, which exploited the glass aptitude to infiltrate a polycrystalline alumina substrate,[7,8,14] was a typical "natural transport based process"[3]; the latter, which built the compositional gradient layer by layer, was a representative "constructive method".[3] While observing the cross-section of each sample, several images were taken and then elaborated, thus obtaining a picture of the entire graded profile, which was then used for the finite element simulations. In order to validate the microstructure based modeling, a systematic micro-indentation test was performed on the cross-section of each FGM, the elastic modulus was deduced by the load–depth indentation curve and the Young's modulus was determined as a function of depth.

2. Materials

2.1. Ingredient materials

Due to their attractive potentialities,[7,8] glass-alumina FGMs were considered in the present research. Both the ingredient materials and the production techniques were described in previous works[15–17] and thus, they are only briefly summarized in the following.

The substrate of both the percolated and the plasma-sprayed samples was made of a commercially available[18] sintered alumina (purity: 99.7%; density: 3.9 g/cm^3; mineralogical composition: α alumina), which was supplied in the form of 5 cm × 5 cm × 0.8 cm tiles. The main mechanical properties of the alumina are reported in Table 1.

In order to produce the FGM by plasma spraying, an alumina powder was required; for this purpose, a commercial product[19] was chosen for its high purity (99.5%) and its grain size, suitable for the plasma spraying process (31 ± 4 μm). Again, only α alumina was detected by the X-ray diffraction in the alumina powder.

The second ingredient material was a glass belonging to the ternary system CaO–ZrO_2–SiO_2 (CZS),[15] which was chosen due to the good thermo-mechanical properties of these glasses.[20,21] In the percolation-based process, the glass was used in bulk form, while in the plasma spraying method the glass was employed in powder form. In the former case, the molten glass was poured into a mould in order to obtain a bar, which was annealed (1 h at 800 °C, slow cooling down inside the kiln) and then cut into 1 mm thick slices; in the latter case, the molten glass was plunged into cold water and the resultant frit was wet ball milled, dried and atomized. The thermo-mechanical properties of the glass are listed in Table 1.

Table 1
Most relevant thermo-mechanical properties of the ingredient materials

	Glass[15]	α-Al_2O_3[17]	β-Al_2O_3[28]
Elastic modulus, E (GPa)	96	380	300
Poisson's coefficient	0.27	0.21	0.27
Coefficient of thermal expansion (K^{-1})	8.7×10^{-6}	8.3×10^{-6}	8.2×10^{-6}

2.2. Functionally graded materials

One type of glass-alumina FGMs was obtained by percolation.[15,16] During the heat treatment (1600 °C, 4 h), the glass melted and progressively penetrated into the polycrystalline alumina, by moving along the grain boundaries and partially filling the residual pores of the substrate. A percolated sample was cut along the infiltration direction in order to study the graded profile. The X-ray energy dispersion spectroscopy (X-EDS), coupled with the scanning electron micrope (SEM), was used to detect the presence of SiO_2, which was considered as a marker of the glass, along the percolation direction; in this way it was possible to estimate the maximum depth reached by the glass. Since the SiO_2 substantially vanished at about 1600 μm of depth, it was assumed that this was the maximum depth reached by the glass.[16] Then the FGM cross-section was carefully polished and subjected to a chemical etching with a 4% fluoridric acid solution for 10 s. Since the chemical treatment removed the glass but did not alter the alumina grains, the microstructural details became evident (Fig. 1). For SEM, several partially overlapped images were taken (in file format) and connected, thus, obtaining a column-like image of the entire graded profile.

The second class of FGMs considered in the present research was obtained by plasma spraying a glass-alumina graded coating onto a sintered alumina substrate,[16,17] previously grit-blasted with SiC powder (mean grain size: 165 μm).[22] Two different compositional profiles were evaluated: in the plasma sprayed sample labeled "FGM-p1" the coating composition varied from

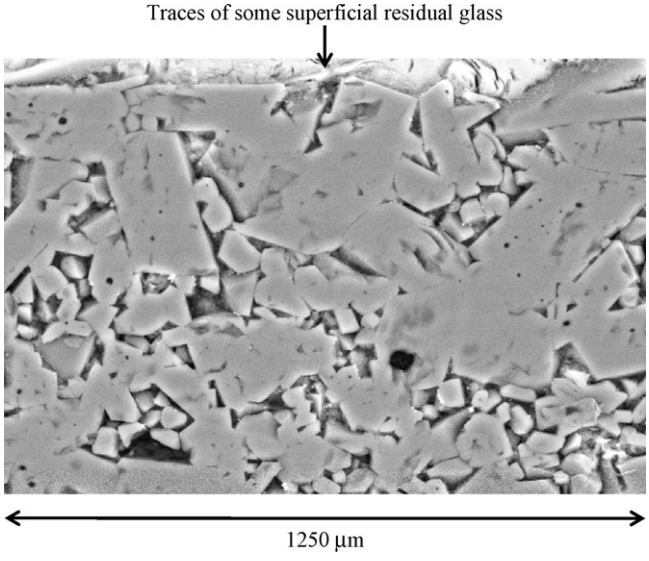

Fig. 1. SEM image of the percolated FGM cross-section after the chemical etching. The picture refers to the upper part of the cross-section.

100% alumina (at the interface with the alumina substrate) to 100% glass (at the top surface), while in the plasma sprayed system named "FGM-p2" the coating composition varied from 80% alumina–20% glass (at the interface with the alumina substrate) to 100% glass (at the top surface), as shown in Fig. 2. In both cases the graded coatings were designed as multilayered systems, in which each layer could be assimilated to a traditional composite material, having a mean composition slightly different from the neighbouring ones. However, both in FGM-p1 and FGM-p2, the layer thickness was minimized (<30 μm), in order to obtain a continuous-like profile, and kept constant. The detailed description of the fabrication process, which employed two separate feeders for the two powders (alumina and glass)[17,23] instead of pre-mixed powder blends,[24–27] and the characterization of the plasma sprayed FGMs were presented in a previous work.[17]

As represented in Fig. 2, the SEM investigation of the cross-sections showed that both in FGM-p1 and FGM-p2 it was not possible to distinguish the deposited layers, since the single layer thickness was comparable with the splat dimension. From this point of view, therefore, the plasma sprayed coatings could be considered as continuously graded systems and not as "stepwise" systems, though they were designed as layered materials. However, if the microscale was considered, the microstructure of the sprayed FGMs was heterogeneous, since the glass and the alumina splats could be clearly discriminated. Moreover, the SEM inspection revealed that the sprayed coatings were characterized by microstructural defects, such as pores and interlamellar cracks; however, the major fault of these coatings in the as-sprayed conditions was the relatively weak interface between the coating and the alumina substrate, as shown in Fig. 2 (detail).

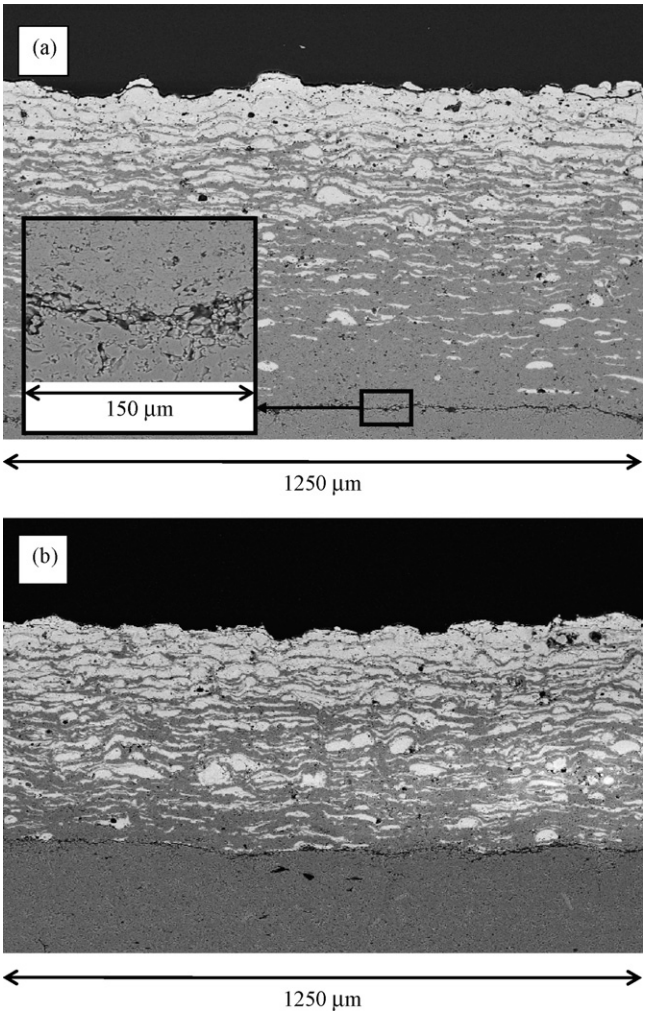

Fig. 2. SEM images of the plasma-sprayed FGMs: (a) FGM-p1, with a detail of the coating–substrate interface; (b) FGM-p2.

Due to the different coating design, though the compositional change rate was the same in the two plasma sprayed systems,[17] the total thickness reached by the coating was higher in FGM-p1 (about 700 μm) than in FGM-p2 (about 500 μm), as proved by the SEM inspection (Fig. 2). As already done for the percolated FGM, during the SEM observation of both the plasma sprayed samples several images of the cross-section were acquired and properly combined, thus obtaining a column-like image of the whole graded region. Since in the FGM-p1 and the FGM-p2 samples the glass splats could be easily identified, it was not necessary to perform a chemical etching to highlight the microstructural features.

3. Methods

3.1. Prediction of the elastic property profile by the rule of mixture

A first attempt to predict the elastic property profile in FGMs was made by applying the rule of mixture (ROM) inspired by the theory of traditional composite materials. In order to do so, the column-like image of the percolated FGM cross-section was elaborated: since the glass had been removed by the chemical etching, the regions originally occupied by the glassy phase were identified, as shown in Fig. 3a, and the residual pores were separately considered as a third phase (along with the glass and the alumina). Then the column-like picture was divided into 16 equal rectangular areas, each of which was about 100 μm high. In each of the 16 areas of the graded profile the volume fractions of the constituent phases were evaluated and the ROM was applied, thus obtaining the mean value of the Young's modulus:

$$E = V_a E_a + V_g E_g + V_p E_p$$

where V_a, V_g and V_p are the volume fractions of the alumina, the glass and the pores in the specific rectangular area considered, while E_a, E_g and E_p are the values of the respective Young's modulus.

The same approach was applied to the plasma sprayed FGMs, with the difference that the glass had not been removed by chemically etching the cross-section and the glass splats were clearly defined. Since the thickness of the graded region was much lower in FGM-p1 and FGM-p2 (about 700 μm and 500 μm, respectively) than in the percolated FGM (about 1600 μm), the column-like pictures of the sprayed samples were divided in fewer rectangular areas, i.e. eight areas for FGM-p1 and six areas for FGM-p2, and the height of each area was reduced

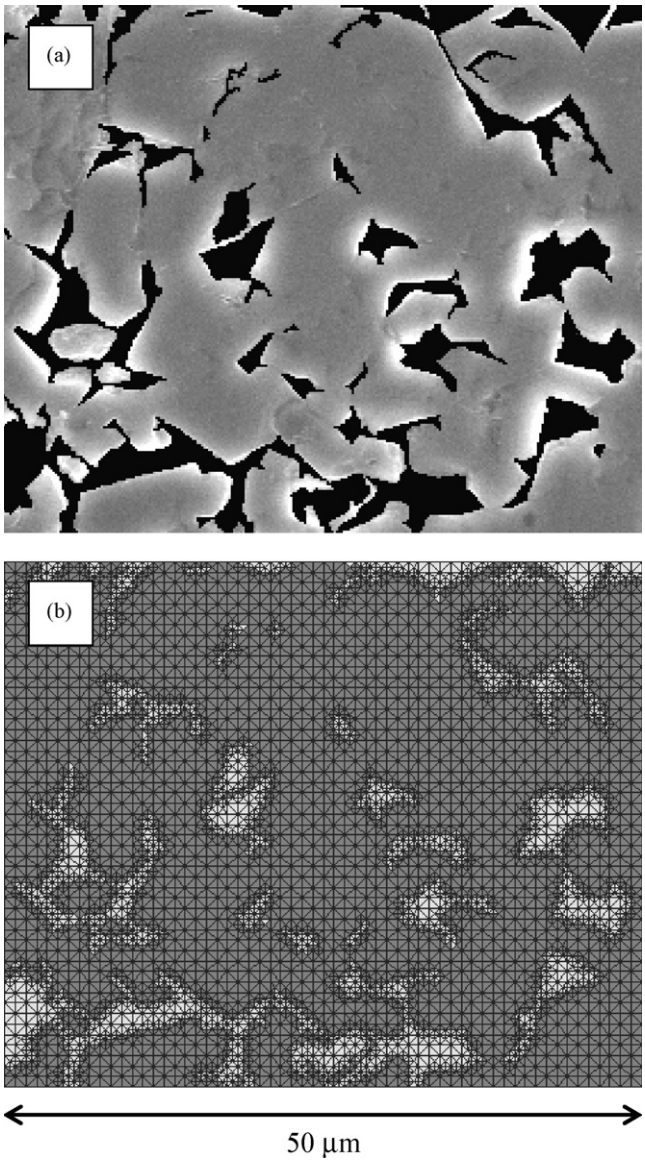

Fig. 3. The picture exemplifies the image elaboration carried out in order to define the area originally occupied by the glass in the percolated FGM cross-section (a) and the respective microstructure-based finite element mesh (b).

from 100 μm to about 85 μm. It is worth noting that the plasma spraying process, while leaving the CZS phase in an amorphous state,[17] caused a wide transformation of the alumina powder from the α to the γ polymorph[17,28] and therefore the α-alumina was not considered in the sprayed samples but it was substituted by the γ-alumina, whose properties, taken from the literature, are listed in Table 1.

3.2. Prediction of the elastic property profile by the finite element method

An alternative way to predict the elastic property profile is represented by the finite element method (FEM). In the present study, the simulations were performed by employing OOF,[29,30] a code which is able to operate on microstructural images and to apply the FEM at the microscale. In fact, pictures (in file format) of the actual microstructure can be acquired and directly mapped onto finite element meshes; the thermo-mechanical properties of the constituent phases can be assigned and used as input data and then OOF can be used to perform virtual tests on the material. Since the simulations are based on images of the real microstructure, OOF is able to reveal the effects of microstructural details such as pores and inclusions and therefore it is a powerful tool to investigate the relation existing between materials properties and microstructure. In fact, OOF has been widely used to investigate complex systems, such as composite materials and FGMs.[31–46] Moreover, OOF has been applied to plasma-sprayed systems: in particular, Wang et al.[47] studied the effect of pores and interfaces on the macroscopic thermo-mechanical properties of plasma-sprayed zirconia coatings, with a special attention to their elastic modulus and thermal conductivity.

As regards the FGMs analysed here, in order to evaluate the elastic modulus as a function of depth the rectangular areas already used for the ROM-based approach were employed. Each area was discretized into a finite element mesh, the properties of the constituent phases were introduced as reported in Table 1, and a test was simulated in order to estimate the elastic modulus. For each area, two different calculations were performed: in the first one, the elastic modulus was calculated along the "*y*" axis, i.e. the axis parallel to the gradient direction; in the second one, the calculation was performed along the "*x*" axis, i.e. the axis perpendicular to the gradient direction (in other words, parallel to the surface). These simulated tensile tests were useful to appreciate the possible local anisotropy of the system. The same procedure was applied to the 16 areas into which the percolated FGM profile was divided, as well as to the 8 areas of the FGM-p1 profile and the 6 areas of the FGM-p2 profile. An example of the microstructure-based meshes, created with triangular elements, is presented in Fig. 3b, which refers to the same area represented in Fig. 3a. Each area of the graded profiles was mapped onto a grid containing about 45,000 elements.

3.3. Experimental measurement of the elastic property profile

In order to validate the values predicted by the ROM and the FEM simulations, the elastic modulus was experimentally measured via depth-sensing micro-indentation (OpenPlatform, CSM Instruments SA). These techniques, in fact, are widely used to quantify not only the hardness, but also the elastic modulus of materials: usually data are collected during a complete cycle of loading and unloading, then unloading data are analysed to obtain the wanted properties.[48] In the present research, the cross-section of the three evaluated systems underwent a systematic Vickers microindentation test, which required to perform several indentations along lines parallel to the "*x*" direction at given depths, as shown in Fig. 4. For each indentation the load–displacement curve was recorded and the local elastic modulus was deduced by applying the Oliver and Pharr's method[48]; then the mean value of the elastic modulus was calculated as an average of the several elastic moduli acquired on each line. In the tests the applied load was set to 10 N for the percolated FGM, but it was reduced to 1 N for the plasma sprayed samples,

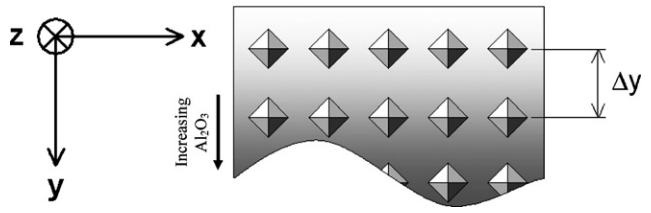

Fig. 4. Exemplifying map of the Vickers microindentation test performed on the cross-section of the three FGMs considered. The interline Δy was set to 100 μm for the percolated FGM and to 85 μm for the sprayed FGM. The indentations were carried out on 16 lines in the percolated FGM, on 8 lines in the FGM-p1 and on 6 lines in the FGM-p2.

which are intrinsically weaker; moreover, the elastic modulus was measured every 100 μm of depth on the percolated FGM cross-section, but it was evaluated every 85 μm of depth on the sprayed specimens, coherently with the height of the correspondent rectangular areas used in the simulations.

4. Results and discussion

As regards the percolated FGM, the analysis of the column-like image revealed that the composition changed along the penetration direction following a substantially linear trend; consequently, as represented in Fig. 5, the elastic modulus predicted by the ROM varied linearly as well, increasing from 330 GPa in the most superficial area to 350 GPa in the deepest area. If compared with the experimental data, the values predicted by the ROM did not fit perfectly, but the difference was of the same order of magnitude as the experimental error. This slight difference could be due to several reasons. First of all, when the ROM was applied within each rectangular area, it was implicitly assumed that the graded system could be locally assimilated to a traditional (not graded) composite material; in other words, the ROM did not account for the compositional change which occurred within the analysed rectangular area. Even more, the ROM was governed by the volume fractions of the constituent phases, but it did not consider such microstructural features as the size and shape of the ingredient materials domains and their actual mutual distribution. Moreover, the ROM was first developed for long fiber composites,[49] while the percolated FGM microstructure was locally similar to a particulate reinforced composite material. However, the relatively good agreement between the calculated values and the experimental ones suggested that the ROM could be reasonably used to evaluate in first approximation the elastic property profile in the percolated specimen. As regards the computational simulations, which faithfully modelled the real microstructure, the calculated values were in good agreement with the elastic properties measured via microindentation, as shown in Fig. 5. It is worth noting that the predicted values of the elastic properties along the "y" axis (parallel to the glass penetration direction) and the "x" axis (perpendicular to the penetration direction) were comparable—in other words, within each rectangular area, E_x was quite similar to E_y. This means that, if the whole graded profile is considered, the glass percolation created a monodirectional gradient and the FGM resulted to be an intrinsically anisotropic system; instead at the microscale, if a local level is considered, i.e. within each rectangular area of the simulation, the material behaviour was proved to be substantially isotropic.

As regards the plasma sprayed samples, the graphs in Fig. 6a and b demonstrate that the ROM could not be validly applied in this case, since the calculated elastic properties were significantly overestimated. In fact, the ROM was not able to account for the abundant microstructural defects which are typical of plasma sprayed systems, such as interlamellar microcracks or

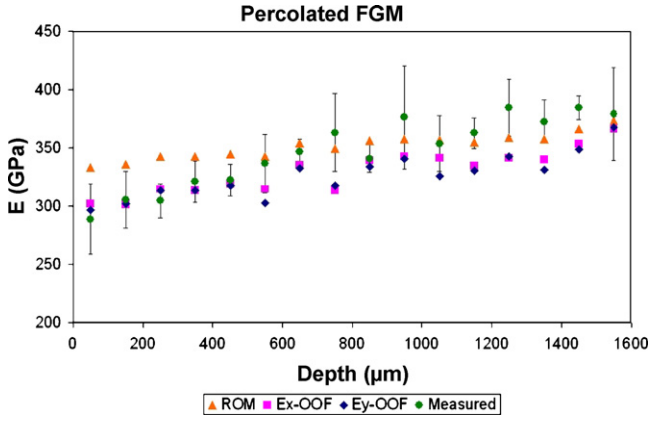

Fig. 5. Comparison between the predicted and the measured elastic properties in the percolated FGM.

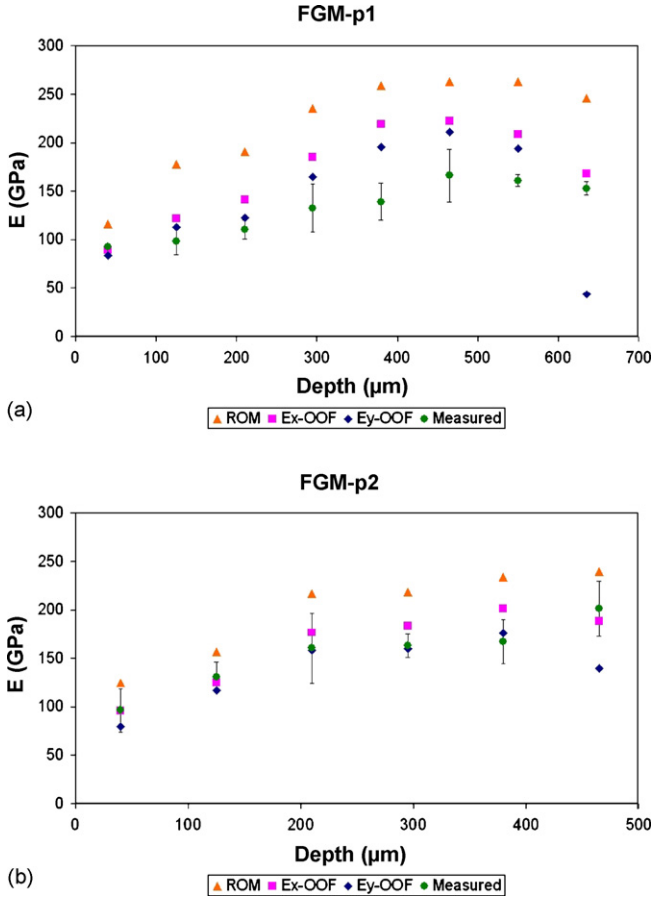

Fig. 6. Comparison between the predicted and the measured elastic properties in the sprayed FGMs.

weak splat–splat interfaces. However, the functional profiles predicted by the ROM were substantially linear for both the sprayed samples, thus confirming the good correspondence between the designed gradients and the fabricated materials. Further information may be obtained by the FEM approach. First of all, the simulations showed that the elastic modulus predicted along the "*y*" direction was systematically lower than the one predicted along the "*x*" direction. As a matter of fact, in the plasma sprayed FGMs two different sources of anisotropy may be identified: the presence of a monodirectional gradient of composition along the "*y*" direction and the peculiar splat-like microstructure generated by the plasma spraying process. In fact, the monodirectional change of composition along the "*y*" axis, which resulted in a functional gradient, caused an anisotropic behaviour which could be appreciated if the dimensional scale of the gradient was considered, as already seen for the percolated FGM. Moreover, during the plasma spraying process, the sprayed particles melted, impacted against the substrate and flattened, creating a lamellar morphology which was inherently anisotropic or, more exactly, transversally isotropic, with isotropy in the plane perpendicular to the spraying direction. This is a well known phenomenon in plasma sprayed materials, since the lamellar shape of splats, which can be assimilated to elongated particles flattened on the substrate plane, as well as the preferential orientation of pores and cracks, which tend to be normal or parallel to the substrate, result in anisotropy of the elastic behaviour[28,47,50] and other properties such as conductivity.[51] Hence, unlike the percolated FGM, the sprayed samples showed an anisotropic behaviour also at the microscale (i.e. within each area of the models). In other words, due to the different microstructures of the examined systems, the anisotropic behaviour of the percolated FGM could be appreciated only if the whole graded profile was considered (typical length scale: hundreds of microns); instead the anisotropic behaviour of the sprayed FGMs could be appreciated also at the microscale, i.e. within each rectangular area of the simulations (typical length scale: tens of microns). Obviously the ROM, which simply accounted for the volume fraction of the constituent phases, could not provide a justifying analysis of this local anisotropy.

Moreover, when comparing the FEM results with the experimental data, it should be noted that the microindentation test was not able to distinguish the "*x*" and "*y*" components of the elastic modulus.[48] Since the elastic displacements occurred primarily in the direction of testing, which was perpendicular to the gradient direction, the measured values should be compared more appropriately with the values predicted along the "*x*" direction than with those predicted along the "*y*" direction[48] (in truth, as shown in Fig. 4, each indentation was performed along the "*z*" direction, but the system could be hypothesized isotropic in the plane "*x*–*z*", which was perpendicular to the gradient direction, as explained before). Nevertheless, the development of the indent during the testing involved deformation in many directions and therefore, the measured modulus could be considered an average quantity.[48] If so, both the calculated values, along the "*x*" and the "*y*" direction, could be compared with the experimental data. On the other hand, several techniques, such as wave velocity analysis[52] and bend test,[53] have been traditionally employed to measure the elastic anisotropy of plasma sprayed materials, but they have been mainly applied to homogeneous materials or traditional (not graded) composites and not to graded coatings. Therefore the depth-sensing indentation technique, in spite of its limitations, resulted to be a good choice because it allowed to measure locally the elastic properties in an easy way.

The graphs in Fig. 6a and b show that the calculated elastic properties generally overestimated the measured ones, though the discrepancy was usually comparable with the experimental error. This discrepancy may be due to the presence of fine microstructural details, which can be hardly included in the model. For example, Damani and Wanner[28] underlined that in plasma-sprayed alumina coatings splats are often discontinuously bonded to each other, thus generating very narrow inter-splat pores. Due to their thinness, such pores at the border of splats could not be clearly distinguished in the SEM images and therefore the simulations overvalued the inter-splat cohesion. In fact, the difference between the calculated and the experimental values was particularly relevant in the central part of the FGM-p1 sample (about 400 μm of depth), where the alumina volume fraction was high and the microstructure appeared particularly dense in the SEM images. Moreover Wang et al.,[47] comparing the effectiveness of OOF and other predictive techniques, recognized that in plasma-sprayed systems the physical properties of splat boundaries cannot be unambiguously defined, which may also cause inaccuracy. Besides this, it should be remarked that also intra-splat cracks and other morphological details of the lamellae may influence the effective properties of the material, but they cannot be fully identified through the image analysis.[47]

In particular, as regards the deepest area in the cross-section of both the sprayed samples, the difference between the calculated values and the experimental data is relevant, especially along the "*y*" axis. This may be due to the fact that, in both cases, the deepest rectangular area considered in the simulations also included the interface between the coating and the substrate which, as already observed, was quite faulty and resembled a bundle of linear cracks preferentially orientated along the "*x*" direction. The predicted values, therefore, were directly affected by the defectiveness of the interface. On the contrary, while performing the experimental measurements, it was not possible to indent exactly on the interface and therefore the acquired data did not strictly refer to the most defective region. By the way, it should be underlined that in the percolated FGM this problem did not arise, since the gradual infiltration of the glass along the grain boundaries did not result in a distinct interface. Actually, the plasma spraying process may be advantageous since it is a constructive technique, which makes it possible to create arbitrarily the compositional gradient and ensures high reproducibility and flexibility; however, the percolation system, which relies on natural transport phenomena, produces thicker glass-alumina coatings (at least with the ingredient materials considered here) and avoids the problems connected with the interface. In order to improve the substrate-coating adhesion of the sprayed FGMs a proper thermal treatment would be required. If the two-sprayed systems are compared, the FGM-p2 sample showed a thinner coating, but the presence of a certain glass fraction (about 20%) in the

region next to the interface improved the adhesion to the substrate, resulting in improved mechanical properties. Moreover, the boundaries between glass splats and alumina splats could be more clearly defined and included in the image-based meshes and therefore FGM-p2, which contained some glass throughout the whole graded coating, could be more carefully modelled.

To conclude, it should be observed that the image-based approach led to an inherently 2D model. The 2D hypothesis may be reasonably applied to the monodirectional FGMs considered here, since they were transversally isotropic systems. However, a 3D simulation could model more faithfully the real material microstructure, which was obviously a 3D structure[45]; in particular, a 3D model could be useful to predict more reliably the behaviour of the interface in the plasma sprayed samples. Nevertheless, in spite of the planar nature of the model, the predicted values were in fairly good agreement with the measured ones.

5. Conclusions

The present research demonstrated the feasibility of producing glass-alumina FGMs via two different techniques, i.e. glass percolation and plasma spraying.[15–17] The former was a natural transport based technique, since it relied on the natural infiltration of a $CaO–ZrO_2–SiO_2$ glass – in the molten state – into a sintered polycrystalline alumina bulk. The latter was a constructive approach, since the gradient was literally built layer by layer; however, though the sprayed FGMs were designed as multi-layered systems, the minimization of the layer thickness allowed to obtain a continuous gradient. The graded zone of the percolated FGM cross-section was much thicker than the sprayed coatings and there was no problem of adhesion; however, the constructive technique ensured higher flexibility and repeatability.

The effective elastic properties of the glass-alumina FGMs were predicted by applying the rule of mixture and using a FEM code which was able to operate at the microscale. With the aim of validating them, the results were compared with the experimental data acquired via microindentation. The ROM could be applied to the percolated FGM, but the result was just a qualitative indication of the elastic profile; moreover, the ROM greatly overestimated the elastic properties of the sprayed samples. Much better results could by obtained by the computational simulations. Actually, some inaccuracies were caused by the difficulty of including the peculiarities of the splat–splat boundaries and other really fine structural details in the model. Nevertheless, the experimental data were fitted fairly well by the microscale computational simulations, which also gave further information about the transversally isotropic behaviour of the FGMs.

Acknowledgements

The present research was partially supported by PRRIITT (Regione Emilia Romagna), Net-Lab "Surface & Coatings for Advanced Mechanics and Nanomechanics" (SUP&RMAN). Many thanks to Centro Sviluppo Materiali (CSM) S.p.A. (Roma, Italy), Surface Engineering Unit, which performed the spraying sessions, and to Ing. Giovanni Bolelli (Dipartimento di Ingegneria dei Materiali e dell'Ambiente, Università di Modena e Reggio Emilia, Italy), who greatly contributed to the graded coatings design. Prof. W.C. Carter and OOF-NIST team are gratefully acknowledged.[29,30]

References

1. Kawasaki, A. and Watanabe, R., Concept and P/M fabrication of functionally graded materials. *Ceramics International*, 1997, **23**, 73–83.
2. Miyamoto, Y., Kaysser, W. A., Rabin, B. H., Kawasaki, A. and Ford, R. G., *Functionally Graded Materials. Design, Processing and Applications*. Kluwer Academic Publishers, 1999.
3. Mortensen, A. and Suresh, S., Functionally graded metals and metal-ceramic composites. I. Processing. *International Materials Review*, 1995, **40**(6), 239–265.
4. Mortensen, A. and Suresh, S., Functionally graded metals and metal-ceramic composites. II. Thermomechanical behaviour. *International Materials Review*, 1997, **42**(3), 85–116.
5. Suresh, S., Modeling and design of multi-layered and graded materials. *Progress in Materials Science*, 1997, **42**, 243–251.
6. Koizumi, M. and Niino, M., Overview of FGM Research in Japan. *MRS Bulletin*, 1995, **1**, 19–21.
7. Jitcharoen, J., Padture, N. P., Giannakopoulos, A. E. and Suresh, S., Hertzian-crack suppression in ceramics with elastic-modulus-graded surfaces. *Journal of the American Ceramic Society*, 1998, **81**(9), 2301–2308.
8. Suresh, S., Olsson, M., Giannakopoulos, A. E., Padture, N. P. and Jitcharoen, J., Engineering the resistance to sliding-contact damage through controlled gradients in elastic properties at contact surfaces. *Acta Materialia*, 1999, **47**(14), 3915–3926.
9. Nakamura, T., Wang, T. and Sampath, S., Determination of properties of graded materials by inverse analysis and instrumented indentation. *Acta materialia*, 2000, **48**, 4293–4306.
10. Grujicic, M. and Zhang, Y., Determination of effective elastic properties of functionally graded materials using Voronoi cell finite element method. *Materials Science and Engineering*, 1998, **A251**, 64–76.
11. Weissenbek, E., Pettermann, H. E. and Suresh, S., Elasto-plastic deformation of compositionally graded metal-ceramic composites. *Acta Materialia*, 1997, **45**(8), 3401–3417.
12. Cannillo, V., Manfredini, T., Corradi, A. and Carter, W. C., Numerical Models of the Effect of Heterogeneity on the Behavior of Graded Materials. *Key Engineering Materials*, 2002, **206–213**, 2163–2166, Trans Tech Publications, Switzerland.
13. Cannillo, V. and Carter, W. C., Numerical models of the effect of elastic heterogeneity on the toughness of graded materials. In *Advances in Fracture Research, Proceedings of ICF10*, ed. K. Ravi-Chandar, B. L. Karihaloo, T. Kishi, R. O. Ritchie, A. T. Yokobori Jr. and T. Yokobori, 2001.
14. Flaitz, P. L. and Pask, J. A., Penetration of polycrystalline alumina by glass at high temperatures. *Journal of the American Ceramic Society*, 1987, **70**(7), 449–455.
15. Cannillo, V., Manfredini, T., Montorsi, M., Siligardi, C. and Sola, A., Glass-alumina functionally graded materials: their preparation and compositional profile evaluation. *Journal of the European Ceramic Society*, 2006, **26**(13), 2685–2693.
16. Cannillo, V., Lusvarghi, L., Manfredini, T., Montorsi, M., Siligardi, C., and Sola, A., Glass-ceramic functionally graded materials produced with different methods, *Journal of the European Ceramic Society*, in press.
17. Cannillo, V., Lusvarghi, L., Manfredini, T., Siligardi, C., and Sola, A., Characterization of glass-alumina functionally graded materials obtained by plasma spraying, *Journal of the European Ceramic Society*, in press.
18. Kéramo ceramiche tecniche, Tavernerio (CO), Italy.
19. Sulzer Metco 105SFP.
20. Leonelli, C. and Siligardi, C., $CaO–SiO_2–ZrO_2$ glasses: modelling and experimental approach. *Recent Research Developments in Materials Science*, 2002, **3**, 599–618.
21. Cannillo, V., de Portu, G., Micele, L., Montorsi, M., Pezzotti, G., Siligardi, C. *et al.*, Microscale computational simulation and experimental measurement of thermal residual stresses in glass-alumina functionally graded

materials. *Journal of the European Ceramic Society*, 2006, **26**(8), 1411–1419.
22. Luciano, Zamboni, Montichiari (BS), Italy (Provider).
23. Vaidya, R. U., Castro, R. G., Peters, M. I., Gallegos, D. E. and Petrovic, J. J., Use of plasma spraying in the manufacture of continuously graded and layered/graded molybdenum disilicide/alumina composites. *Journal of Thermal Spray Technology*, 2002, **11**(3), 409–414.
24. Gu, Y. W., Khor, K. A., Fu, Y. Q. and Wang, Y., Functionally graded ZrO_2–NiCrAlY coatings prepared by plasma spraying using pre-mixed, spheroidized powders. *Surface and Coatings Technology*, 1997, **96**, 305–312.
25. Xinhua, X., Jingchuan, Z., Zhongda, Y. and Zhonghong, L., Fabrication and microstructure of ZrO_2/NiCrCoAlY graded coating by plasma spraying. *Surface and Coatings Technology*, 1996, **88**, 66–69.
26. Khor, K. A., Gu, Y. W. and Dong, Z. L., Plasma spraying of functionally graded yttria stabilized zirconia/NiCoCrAlY coating system using composite powders. *Journal of Thermal Spray Technology*, 2000, **9**(2), 245–249.
27. Yan, D., He, J., Li, X., Liu, Y., Dong, Y. and Liu, H., The corrosion behavior of plasma-sprayed Ni/Al–Al_2O_3 and Ni/Al–Al_2O_3 + 13 wt.% TiO_2 graded ceramic coatings in 5% HCl solution. *Surface and Coatings Technology*, 2003, **176**, 30–36.
28. Damani, R. J. and Wanner, A., Microstructure and elastic properties of plasma-sprayed alumina. *Journal of materials science*, 2000, **35**, 4307–4318.
29. Carter, W.C., Langer, S.A., Fuller Jr., E.R., *The OOF Manual*, version 1.0, 1998.
30. Langer, S. A., Fuller Jr., E. R. and Carter, W. C., OOF: an image-based finite element analysis of material microstructures. *Computing in Science and Engineering*, 2001, **3**, 15–23.
31. Hsueh, C. H., Fuller Jr., E. R., Langer, S. A. and Carter, W. C., Analytical numerical analyses for two-dimensional stress transfer. *Materials Science and Engineering A*, 1999, **268**(1/2), 1–7.
32. Hsueh, C. H., Haynes, J. A., Lance, M. J., Becher, P. F., Ferber, M. K., Fuller Jr., E. R. *et al.*, Effects of interface roughness on residual stresses in thermal barrier coatings. *Journal of the American Ceramic Society*, 1999, **82**(4), 1073–1075.
33. Hsueh, C. H. and Fuller Jr., E. R., Residual stresses in thermal barrier coating: effects of interface asperity curvature/height and oxide thickness. *Materials Science and Engineering A*, 2000, **283**(1/2), 46–55.
34. Zimmermann, A., Fuller Jr., E. R. and Rödel, J., Residual stress distributions in ceramics. *Journal of the American Ceramic Society*, 1999, **82**(11), 3155–3160.
35. Zimmermann, A., Carter, W. C. and Fuller Jr., E. R., Damage evolution during microcracking of brittle solids. *Acta Materialia*, 2001, **49**(1), 127–137.
36. Zimmerman, M. H., Baskin, D. M., Faber, K. T., Fuller Jr., E. R., Allen, A. J. and Keane, D. T., Fracture of a textured anisotropic ceramic. *Acta Materialia*, 2001, **49**(16), 3231–3242.
37. Vedula, V. R., Glass, S. J., Saylor, D. M., Rohrer, G. S., Carter, W. C., Langer, S. A. *et al.*, Residual-stress predictions in polycrystalline alumina. *Journal of the American Ceramic Society*, 2001, **84**(12), 2947–2954.
38. Saigal, A., Fuller Jr., E. R., Langer, S. A., Carter, W. C., Zimmerman, M. H. and Faber, K. T., Effect of interface properties on microcracking of iron titanate. *Scripta Materialia*, 1998, **38**(9), 1453–1499.
39. Saigal, A. and Fuller Jr., E. R., Analysis of stresses in aluminium–silicon alloys. *Computational Materials Science*, 2001, **21**(1), 149–158.
40. Cannillo, V. and Carter, W. C., Computation and simulation of reliability parameters and their variations in heterogeneous materials. *Acta Materialia*, 2000, **48**(13), 3593–3605.
41. Cannillo, V., Leonelli, C., Manfredini, T., Montorsi, M. and Boccaccini, A. R., Computational simulations for the assessment of the mechanical properties of glass with controlled porosity. *Journal of Porous Materials*, 2003, **10**(3), 189–200.
42. Cannillo, V., Leonelli, C. and Boccaccini, A. R., Numerical models for thermal residual stresses in Al_2O_3 platelets/borosilicate glass matrix composites. *Materials Science and Engineering*, 2002, **A323**, 246–250.
43. Cannillo, V., Corradi, A., Leonelli, C. and Boccaccini, A. R., A simple approach for determining the in situ fracture toughness of ceramic platelets used in composite materials by numerical simulations. *Journal of Materials Science Letters*, 2001, **20**, 1889–1891.
44. Cannillo, V., Pellacani, G. C., Leonelli, C. and Boccaccini, A. R., Numerical modeling of the fracture behavior of a glass matrix composite reinforced with alumina platelets. *Composites Part A*, 2003, **34**, 43–51.
45. Cannillo, V., Manfredini, T., Montorsi, M. and Boccaccini, A. R., Investigation of the mechanical properties of Mo-reinforced glass-matrix composites. *Journal of Non-Crystalline Solids*, 2004, **344**, 88–93.
46. Cannillo, V., Manfredini, T., Montorsi, M., Siligardi, C. and Sola, A., Microstructure-based modelling and experimental investigation of crack propagation in glass-alumina functionally graded materials. *Journal of the European Ceramic Society*, 2006, **26**(15), 3067–3073.
47. Wang, Z., Kulkarni, A., Deshpande, S., Nakamura, T. and Herman, H., Effects of pores and interfaces on effective properties of plasma sprayed zirconia coatings. *Acta Materialia*, 2003, **51**, 5319–5334.
48. Oliver, W. C. and Pharr, G. M., An improved technique for determining hardness and elastic modulus using load and displacement sensing indentation experiments. *Journal of Materials Research*, 1992, **7**(6), 1564–1583.
49. Gibson, R. F., *Principles of Composite Material Mechanics*. McGraw-Hill International Editions, 1994.
50. Sevostianov, I., Kachanov, M., Ruud, J., Lorraine, P. and Dubois, M., Quantitative characterization of microstructures of plasma-sprayed coatings and their conductive and elastic properties. *Materials Science & Engineering*, 2004, **A386**(1/2), 164–174.
51. Bolelli, G., Cannillo, V., Lusvarghi, L., Manfredini, T. and Montorsi, M., Glass alumina composite coatings by plasma spraying. Part II: microstructure-based modelling of mechanical properties. *Surface and Coatings Technology*, 2006, **201**, 474–486.
52. Wanner, A. and Lutz, E. H., Elastic anisotropy of plasma-sprayed, free-standing ceramics. *Journal of the American Ceramic Society*, 1998, **81**(10), 2706–2708.
53. Hyung-Jun, K. and Young-Gak, K., Elastic modulus of plasma-sprayed coatings determined by indentation and bend tests. *Thin Solid Films*, 1999, **342**(1/2), 201–206.